

# MedMerge: Merging Models for Effective Transfer Learning to Medical Imaging Tasks

Ibrahim Almakky, Santosh Sanjeev, Anees Ur Rehman Hashmi, Mohammad Areeb Qazi, and Mohammad Yaqub

Mohamed bin Zayed University of Artificial Intelligence, Abu Dhabi, UAE  
`{firstname.lastname}@mbzuai.ac.ae`

**Abstract.** Transfer learning has become a powerful tool to initialize deep learning models to achieve faster convergence and higher performance. This is especially useful in the medical imaging analysis domain, where data scarcity limits possible performance gains for deep learning models. Some advancements have been made in boosting the transfer learning performance gain by merging models starting from the same initialization. However, in the medical imaging analysis domain, there is an opportunity in merging models starting from different initialization, thus combining the features learnt from different tasks. In this work, we propose MedMerge, a method whereby the weights of different models can be merged, and their features can be effectively utilized to boost performance on a new task. With MedMerge, we learn kernel-level weights that can later be used to merge the models into a single model, even when starting from different initializations. Testing on various medical imaging analysis tasks, we show that our merged model can achieve significant performance gains, with up to 3% improvement on the  $F_1$  score. The code implementation of this work will be available at [www.github.com/BioMedIA-MBZUAI/MedMerge](http://www.github.com/BioMedIA-MBZUAI/MedMerge).

**Keywords:** Model Merging · Transfer Learning · Medical Image Analysis · Weight Averaging

## 1 Introduction

A good model initialization plays a critical role in the training and performance of deep learning models. To this end, transfer learning has been established as an effective strategy to boost overall model performance, especially when dealing with small datasets such as the ones available in medical settings [19]. Despite differences in the nature of tasks and imaging modalities, ImageNet [10] has proven to be an effective initialization for many medical imaging tasks [6,17]. The gain in performance is largely due to feature re-use, where the weights learned in the source domain result in features that can readily be used in the target domain [17]. Intuitively, transfer learning from a model pre-trained on similar medical imaging tasks that share the same modality and pathology with the downstream task should yield higher performance gains [23,5]. However,

successful transfer learning requires a reasonably large and diverse set of images, prompting efforts to collate large amounts of medical data to effectively pre-train deep learning models [18]. However, for medical imaging problems, collating such large amounts of data is often infeasible due to challenges related to data privacy and the availability of expert annotation.

Model merging has garnered increased attention due to practical possibilities for resource-saving and overcoming data privacy concerns [22,12]. Furthermore, with the promise of removing dependence on a single pre-trained model, the merging of model weights can reduce the tendency of a single model to overfit particular samples, thus improving the accuracy, diversity, and robustness of predictions [13]. Model weight averaging [21] is the most direct, simple, and efficient approach to combining several models and has been used effectively in collaborative learning paradigms. However, simple weight averaging can lead to some bias when large differences are present between the pre-training tasks. Models Soups [22] implements a greedy algorithm to select fine-tuned models to be merged following a hyperparameter search. The selected models are then aggregated using simple weight averaging, often yielding promising performance gains. However, even if overlooking the computational cost associated with such an extensive search of the hyperparameter space, the Model Soups approach [22] focuses on merging models starting from the same initialization. In medical imaging analysis contexts, it is important to benefit from models that have been pre-trained on different tasks, thus harnessing their capacity for another downstream task. Another approach to model merging, dubbed Fisher Merging, has been proposed to choose parameters that approximately maximize the joint likelihood of the posteriors of models' parameters [16]. However, they also focus on models starting from the same initialization as Fisher Merging is less performant when applied to models far apart in the parameter space.

In this work, we focus on the medical imaging analysis domain and consider the need to start from models with different initializations. Therefore, we propose MedMerge to effectively utilize features learnt from various tasks. MedMerge can learn kernel-level weights to carry out a weighted average merge of model weights from different initializations, thus learning how to effectively combine features from previous pertaining tasks. The key contributions of this work can be summarized as follows:

- We propose a novel method, dubbed MedMerge, to merge models pre-trained on different datasets while effectively utilizing features from different models.
- We empirically demonstrate our proposed approach's effectiveness on various medical imaging analysis tasks and show significant performance gains.
- We provide insights into the layer-wise feature transfer from source initializations to target tasks and show a correlation between the selection ratio from specific initializations and the performance gain achieved in an ordinary transfer learning setting.

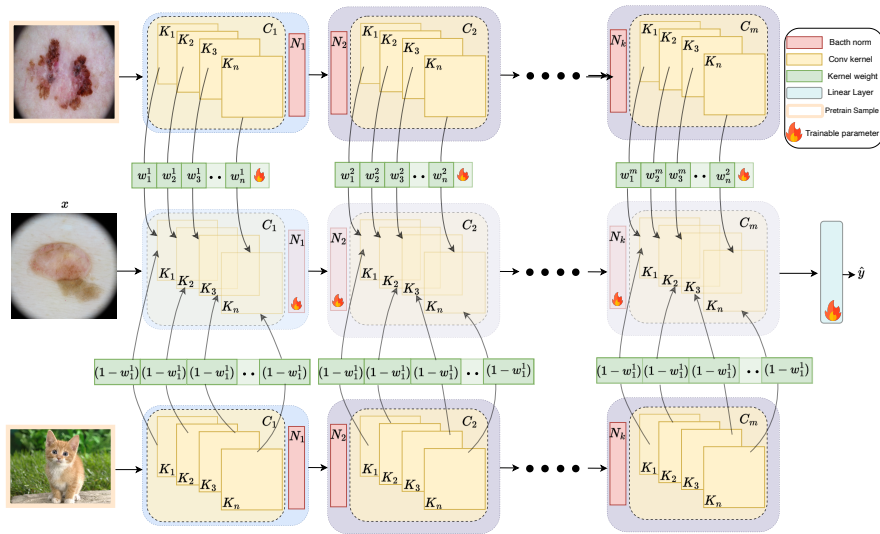


**Fig. 1.** The proposed MedMerge linear probing stage when the kernel-based weighted average vectors are learnt from two pre-trained backbones on two different tasks. The training using the linear probe ensures that frozen features from both backbones are combined effectively to be more separable in the latent representation space.

## 2 Methodology

**Problem formulation.** Let  $M$  be a model composed of a feature extraction backbone  $B$  and a classification head  $H$ . The backbone feature extractor  $B$  is a Convolutional Neural Network (CNN) with a set of convolutional layers  $C \in \{C_1 \dots, C_m\}$ . Each layer  $C$  having a set of kernels  $K = \{K_1, \dots, K_n\}$ , followed by an activation function. The backbone also has a set of batch normalization layers  $\{N_1, \dots, N_k\}$ . On the other hand, the classification head  $H$  is a fully-connected layer that takes the features extracted by  $B$  as input and outputs the model predictions. We also consider  $\theta_B^{(i)}$  and  $\theta_H^{(i)}$  as the backbone and classification head parameters obtained by training model  $M$  on dataset  $D_i$ . This means that the learnt parameters for the convolutional kernel  $K_j$  and batch normalization layer  $N_j$  can be represented as  $\theta_{K_j}^{(i)}$  and  $\theta_{N_j}^{(i)}$ , respectively.

**MedMerge.** In this work, we propose MedMerge, a method to effectively combine the weights of a set of feature extractors  $\Theta = \{\theta_B^{(1)}, \dots, \theta_B^{(d)}\}$ , where each  $\theta_i \in \Theta$  has been obtained by pre-training the model architecture  $M$  on dataset  $D_i \in \{D_1, \dots, D_d\}$ . The combined weights will then form  $\hat{\theta}^{(q)}$ , the effectiveness of which is determined by the performance gains when fine-tuned on unseen dataset  $D_q \notin \{D_1, \dots, D_d\}$ . To accomplish this, we introduce a set of learnt weight parameters  $W = \{w_1, \dots, w_n\}$ , where each weight parameter  $w_j$  corresponds to a kernel  $K_j$  in the CNN backbone  $B$ . Those weights are then used

to form the convolutional kernels in  $\hat{\theta}^{(q)}$ , where each kernel is formed as follows:  $\hat{\theta}_{K_j}^{(q)} = w_j\theta_{K_j}^{(b)} + (1 - w_j)\theta_{K_j}^{(c)}$ , where  $\theta^b$  and  $\theta^c$  are the parameters of  $M$  after pre-training on datasets  $D_b$  and  $D_c$ , respectively. [11] showed that full fine-tuning distorts the pre-trained features and that linear probing a model before fine-tuning (LP-FT) provides a good initialization for the classification head. Furthermore, due to its limited capability, the linear probe depends heavily on the class separability in the latent feature space, making it useful for evaluating feature generalization [2]. Therefore, in MedMerge, we employ a linear probing strategy, depicted in Fig. 1, by freezing the weights of the models that are being combined while using the gradients from the linear probe to learn  $W$ . This means that  $w_j$  is updated based on the gradients for the combined kernels  $K_j^{(b)}$  and  $K_j^{(c)}$  from both models.

Batch normalization [7] plays a critical role when training deep learning models. Specifically for model merging, [14] demonstrated the effectiveness of local batch normalization in alleviating the feature shift between client models in federated learning settings and the impact that has on model aggregation. Thus, in MedMerge, we initialize the batch normalization layers for  $\theta$  as the mean of the corresponding layers in the aggregated models. Then, unlike frozen convolutional kernels, the batch normalization layers are left unfrozen during the linear probing stage.

### 3 Experimental Setup

**Datasets.** We select medical imaging datasets with various modalities and pathologies to adequately assess the efficacy of our approach in comparison with other transfer learning approaches. As such, we select three pairs of datasets that share modality and pathology, which are:

- HAM10K [20] and ISIC-2019 [3]: Skin lesion datasets with 11, 720 and 25, 331 images, respectively. The HAM10K dataset contains 7 classes of lesions, while ISIC-2019 contains 8 classes. We use the official train, validation, and testing split for the HAM10K dataset, while we use a random 60%, 20%, and 20% split for the same sets of the ISIC-2019 dataset.
- EyePACS [4] and APTOS [9]: Diabetic retinopathy datasets with 88, 702 and 3, 962 images, respectively. The two datasets consist of five classes representing the increasing severity of diabetic retinopathy. Since the testing data is not publicly available, we follow a random 80%, 10%, and 10% split for training, validation, and testing, respectively.
- CheXpert [8] and RSNA pneumonia [1]: Chest X-ray datasets with 191, 747 and 14, 863 images, respectively. The CheXpert dataset has 13 pathologies and is a multi-label dataset, whereas the RSNA Pneumonia has two classes representing the presence and absence of Pneumonia. For the CheXpert dataset, we follow the official train, validation and testing split, whereas for the RSNA Pneumonia dataset, we follow an 80%, 10%, and 10% split for training, validation, and testing, respectively.

**Implementation details.** As widely used deep CNN architectures, we primarily use DenseNet-121 and ResNet-50 as the backbones for all our experiments, with the results for ResNet-50 reported in Appendix A1. We have two training regimes, one for LP and the other during fine-tuning, which are used for MedMerge and LP-FT. For LP, we use random initialization for the fully-connected layer of the classification head. We train the model by minimizing the cross entropy loss using the AdamW optimizer [15] with a learning rate of  $10^{-4}$  for 50 epochs. We also minimize the cross entropy loss during full fine-tuning using the AdamW optimizer, but we decrease the learning rate to  $10^{-5}$ , and maintain the number of epochs at 50. All models pre-trained on ImageNet have been specifically trained using ImageNet1K. The models pre-trained on HAM10K, EyePACS, and CheXpert were initialized from ImageNet1K pre-trained parameters. In MedMerge, the kernel-based weights are initialized to a value of 0.5, which provides an equal merge between the features of the two models. All input images are resized to  $224 \times 224$ , and to reduce variance between experiments, we do not conduct any data augmentation strategies during LP or fine-tuning. All models were trained and tested using NVIDIA A5000 GPUs. The full code, hyperparameters, and dataset splits will be available at: [www.github.com/BioMedIA-MBZUAI/MedMerge](http://www.github.com/BioMedIA-MBZUAI/MedMerge).

## 4 Results and Analysis

In Table 1, we compare the performance of MedMerge with that of LP-FT [11] and full Fine-Tuning (FT). We observe that our merging approach outperforms direct fine-tuning as well as LP-FT, with significant performance gains on the transfer case from ImageNet and EyePACS to APTOS. We focus on the macro-averaged  $F_1$  score as it can better assess the performance of the models with the presence of significant class imbalance, especially in the case of the ISIC-2019 dataset. We can clearly observe the impact of MedMerge’s ability to combine the features from the different initializations effectively. Moreover, we notice a smaller gain in performance with the RSNA pneumonia dataset, where even the performance achieved with FT is high. In the case of RSNA pneumonia, the model generalization from training and validation to testing is more challenging in the push to the maximum performance value. As described in [11], we observe increased performance using LP-FT compared to FT. The RSNA pneumonia case is the only one where FT outperforms LP-FT when transferring from ImageNet. It is important to note that we also conducted experiments using ResNet-50 as the backbone and achieved similar performance gains to those reported in Table 1 and are reported in Appendix A1.

Gaining a better understanding of features transferred from source tasks to a target task during our MedMerge LP stage, we analyse the kernel-based weights learned during the LP stage at the layer level. We can clearly observe that the overall shift in the weight selection between the two source tasks in Fig. 2 corresponds with better FT performance in Table 1. More specifically, in the ISIC-2019 and APTOS cases, the kernel-based weights are higher for the

**Table 1.** Comparison between the performance achieved by our learnt kernel-based averaging method and other transfer learning methods on the test sets of ISIC-2019, APTOS, and RSNA-Pneumonia datasets.

Approach	Source	Target	Acc.	$F_1$
FT	ImageNet	ISIC-2019	0.805	0.685
FT	HAM10K	ISIC-2019	0.810	0.699
LP-FT	ImageNet	ISIC-2019	0.777	0.638
LP-FT	HAM10K	ISIC-2019	0.821	0.705
MedMerge (Ours)	ImageNet+HAM10K	ISIC-2019	<b>0.814</b>	<b>0.714</b>
FT	ImageNet	APTOS	0.826	0.639
FT	EyePACS	APTOS	0.834	0.673
LP-FT	ImageNet	APTOS	0.823	0.650
LP-FT	EyePACS	APTOS	0.831	0.687
MedMerge (Ours)	ImageNet+EyePACS	APTOS	<b>0.842</b>	<b>0.713</b>
FT	ImageNet	RSNA-Pneumonia	0.949	0.946
FT	CheXpert	RSNA-Pneumonia	0.935	0.932
LP-FT	ImageNet	RSNA-Pneumonia	0.947	0.944
LP-FT	CheXpert	RSNA-Pneumonia	0.946	0.944
MedMerge (Ours)	ImageNet+CheXpert	RSNA-Pneumonia	<b>0.950</b>	<b>0.947</b>

datasets sharing the modality with the target, i.e. HAM10K and APTOS, respectively. Inversely, for RSNA pneumonia, the kernel-based weights are higher for ImageNet, reflected in the FT performance in Table 1. Moreover, the heatmaps show more weight assigned to layers in the deeper parts of either of the source models towards the linear probe. Intuitively, this means that the more abstract features at the end of the model need to belong to a dominant pertaining task. We can see the manifestation of this in Fig. 3, where low-level features require much less adaptation compared to their high-level counterparts. This further highlights the importance of applying different weights at different model layers, and shows the effectiveness of the learnt MedMerge weights.

**Computational cost.** The computational cost associated with a parameter-level weighted averaging approach can be high, mainly because of the additional weight parameters required and the training process that entails computing gradients on the new target data. Therefore, in MedMerge, we opt for kernel-level learnt weights rather than parameter level. This offers a lighter-weight solution while enabling the effective combination of kernels from different models. We also conducted tests while learning parameter-level weights between the two initializations, but they did not yield any gain in performance when compared with kernel-level weights. This is likely because the changes required to adapt the kernels from the different initializations do not require intricate adaptations. This might be different in cases where there are extreme differences between the source initializations. Furthermore, learning the kernel-level weights is only required during the MedMerge LP stage, after which we can use the learnt weights

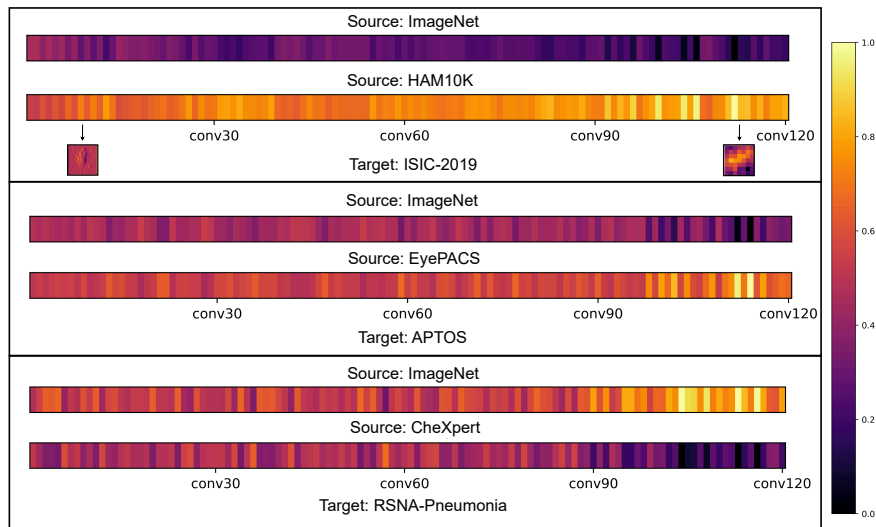


**Fig. 2.** A depth-wise heatmap showing the mean of learnt kernel-based weights at every convolutional layer of the DenseNet-121 backbone. This shows the learned kernel-level weights for the three target datasets: ISIC-2019, APTOS, and RSNA Pneumonia.

to combine the models before moving on to the fine-tuning process. This means that the only difference in computation between MedMerge and LP-FT is the weighted average computation during the LP stage.

**Batch normalization.** In Section 2, we discussed the role of batch normalization layers within MedMerge, highlighting the importance of keeping the batch normalization layers unfrozen during the MedMerge LP stage. We conducted an ablation study to verify this role, leaving the batch normalization layers frozen during the MedMerge LP stage. This led to a drop in the performance achieved by the model during both the LP and FT stages. This implies that the mean of the batch normalization layers from the two source initializations is less effective for the target task.

**Combining with zeros.** To better understand the kernel-level weights learned by MedMerge, we analyse the learnt weights when combining a source initialization with a zeros initialization. It is known that zero initialization will not contribute to extracting meaningful features from the target dataset, which implies that learning to pick zeros over a feature is likely because that feature is detrimental. In such way, in Fig. 4 we can see a pattern of deeper layers where the kernel-level weights are alternating towards the non-zero initialization. The alternating pattern can be attributed to the nature of the blocks in the DenseNet-121 backbone. This further supports the argument regarding the importance of difference merge weights between layers.

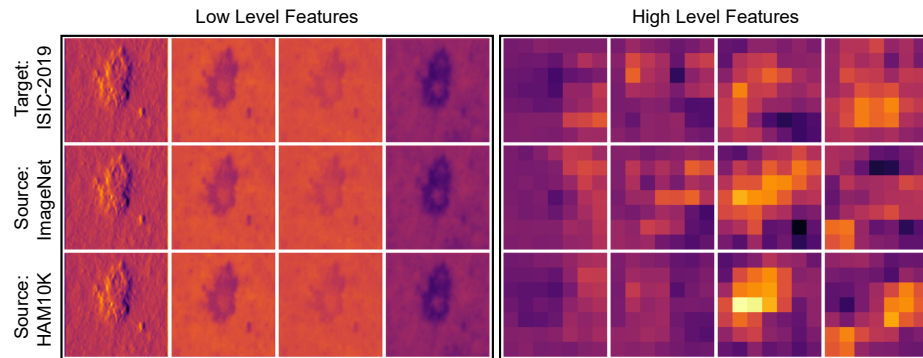


**Fig. 3.** Visualization of the low and high level features for an image sample from the ISIC-2019 when passed through two source models and merged model using MedMerge.

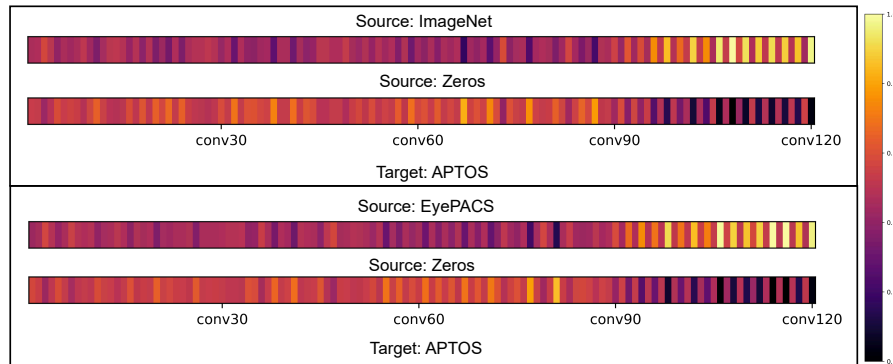


**Fig. 4.** A depth-wise heatmap showing the mean of learnt kernel-based weights at every convolutional layer of the DenseNet-121 backbone when merging between one of the source initializations and zeros towards APTOS.

## 5 Conclusions and Future Work

We address an important opportunity in the medical imaging analysis domain: to use features learned from models pre-trained on different tasks to help boost performance on a target task. To accomplish this, we propose MedMerge to merge models starting from different initializations effectively. In MedMerge, we show that learning kernel-level weights to combine models from different initializations results in a merged model that can outperform the performance achieved by fine-tuning (FT) or linear probing and then fine-tuning (LP-FT). We demonstrate the performance gains of MedMerge on various medical imaging analysis tasks and conduct layer-wise analysis of the merging process. We conclude that this work mainly focuses on CNN backbones, but in the future, we intend to investigate this aggregation approach in Transformer-based architec-

ture. Furthermore, in the future, it would be important to investigate the best approaches to combining more than two model initializations simultaneously.

## References

1. Anouk, S., Carol, W., et al.: Rsnna pneumonia detection challenge (2018), <https://kaggle.com/competitions/rsna-pneumonia-detection-challenge>
2. Asano, Y.M., Vedaldi, A., Rupprecht, C.: A critical analysis of self-supervision, or what we can learn from a single image. Proceedings of the ICLR 2020 (Mar 2020), <https://ora.ox.ac.uk/objects/uuid:6a3bcf03-9360-433f-9dbf-3a6814a32412>
3. Combalia, M., Codella, N.C.F., Rotemberg, V., Helba, B., Vilaplana, V., Reiter, O., Carrera, C., Barreiro, A., Halpern, A.C., Puig, S., Malvey, J.: BCN20000: Dermoscopic Lesions in the Wild. arXiv e-prints p. arXiv:1908.02288 (Aug 2019). <https://doi.org/10.48550/arXiv.1908.02288>
4. Dugas, E., Jorge, J., Cukierski, W.: Diabetic retinopathy detection (2015), <https://kaggle.com/competitions/diabetic-retinopathy-detection>
5. Ghesu, F.C., Georgescu, B., Mansoor, A., Yoo, Y., Neumann, D., Patel, P., Vishwanath, R.S., Balter, J.M., Cao, Y., Grbic, S., Comaniciu, D.: Self-supervised Learning from 100 Million Medical Images. arXiv e-prints p. arXiv:2201.01283 (Jan 2022). <https://doi.org/10.48550/arXiv.2201.01283>
6. Huh, M., Agrawal, P., Efros, A.A.: What makes imagenet good for transfer learning? (Dec 2016), <http://arxiv.org/abs/1608.08614>, arXiv:1608.08614 [cs]
7. Ioffe, S., Szegedy, C.: Batch Normalization: Accelerating Deep Network Training by Reducing Internal Covariate Shift. arXiv (Feb 2015). <https://doi.org/10.48550/arXiv.1502.03167>
8. Irvin, J., Rajpurkar, P., Ko: CheXpert: A Large Chest Radiograph Dataset with Uncertainty Labels and Expert Comparison. arXiv (Jan 2019). <https://doi.org/10.48550/arXiv.1901.07031>
9. Karthik, Maggie, S.D.: Aptos 2019 blindness detection (2019), <https://kaggle.com/competitions/aptos2019-blindness-detection>
10. Krizhevsky, A., Sutskever, I., Hinton, G.E.: ImageNet Classification with Deep Convolutional Neural Networks. Advances in Neural Information Processing Systems **25** (2012), <https://proceedings.neurips.cc/paper/2012/hash/c399862d3b9d6b76c8436e924a68c45b-Abstract.html>
11. Kumar, A., Raghunathan, A., Jones, R., Ma, T., Liang, P.: Fine-Tuning can Distort Pretrained Features and Underperform Out-of-Distribution. International Conference on Learning Representations (Jan 2022), <https://par.nsf.gov/biblio/10337813>
12. Li, W., Peng, Y., Zhang, M., Ding, L., Hu, H., Shen, L.: Deep Model Fusion: A Survey. arXiv (Sep 2023). <https://doi.org/10.48550/arXiv.2309.15698>
13. Li, X., Jiang, M., Zhang, X., Kamp, M., Dou, Q.: FedBN: Federated Learning on Non-IID Features via Local Batch Normalization (May 2021), <http://arxiv.org/abs/2102.07623>, arXiv:2102.07623 [cs]
14. Li, X., Jiang, M., Zhang, X., Kamp, M., Dou, Q.: Fed{bn}: Federated learning on non- $\{iid\}$  features via local batch normalization. In: International Conference on Learning Representations (2021), <https://openreview.net/pdf?id=6YEQUn0QICG>
15. Loshchilov, I., Hutter, F.: Decoupled Weight Decay Regularization. arXiv e-prints p. arXiv:1711.05101 (Nov 2017). <https://doi.org/10.48550/arXiv.1711.05101>

16. Matena, M.S., Raffel, C.A.: Merging Models with Fisher-Weighted Averaging. *Advances in Neural Information Processing Systems* **35**, 17703–17716 (Dec 2022), [https://proceedings.neurips.cc/paper\\_files/paper/2022/hash/70c26937fbf3d4600b69a129031b66ec-Abstract-Conference.html](https://proceedings.neurips.cc/paper_files/paper/2022/hash/70c26937fbf3d4600b69a129031b66ec-Abstract-Conference.html)
17. Matsoukas, C., Haslum, J.F., Sorkhei, M., Soderberg, M., Smith, K.: What Makes Transfer Learning Work for Medical Images: Feature Reuse & Other Factors (Jun 2022). <https://doi.org/10.1109/CVPR52688.2022.00901>, <https://ieeexplore.ieee.org/document/9878482/>
18. Mei, X., Liu, Z., Robson, P.M., Marinelli, B., Huang, M., Doshi, A., Jacobi, A., Cao, C., Link, K.E., Yang, T., Wang, Y., Greenspan, H., Deyer, T., Fayad, Z.A., Yang, Y.: RadImageNet: An Open Radiologic Deep Learning Research Dataset for Effective Transfer Learning. *Radiology: Artificial Intelligence* **4**(5), e210315 (Sep 2022). <https://doi.org/10.1148/ryai.210315>, <https://pubs.rsna.org/doi/10.1148/ryai.210315>, publisher: Radiological Society of North America
19. Raghu, M., Zhang, C., Kleinberg, J., Bengio, S.: Transfusion: Understanding Transfer Learning for Medical Imaging (Oct 2019), <http://arxiv.org/abs/1902.07208>, arXiv:1902.07208 [cs, stat]
20. Tschandl, P., Rosendahl, C., Kittler, H.: The HAM10000 dataset, a large collection of multi-source dermatoscopic images of common pigmented skin lesions. *Sci. Data* **5**(180161), 1–9 (Aug 2018). <https://doi.org/10.1038/sdata.2018.161>
21. Wang, H., Yurochkin, M., Sun, Y., Papailiopoulos, D., Khazaeni, Y.: Federated Learning with Matched Averaging. *International Conference on Learning Representations* (Apr 2020), <https://par.nsf.gov/biblio/10183696>
22. Wortsman, M., Ilharco, G., Gadre, S.Y., Roelofs, R., Gontijo-Lopes, R., Morcos, A.S., Namkoong, H., Farhadi, A., Carmon, Y., Kornblith, S., Schmidt, L.: Model soups: averaging weights of multiple fine-tuned models improves accuracy without increasing inference time. In: *Proceedings of the 39th International Conference on Machine Learning*. pp. 23965–23998. PMLR (Jun 2022), <https://proceedings.mlr.press/v162/wortsman22a.html>, ISSN: 2640-3498
23. Xie, Y., Richmond, D.: Pre-training on Grayscale ImageNet Improves Medical Image Classification (2018), [https://openaccess.thecvf.com/content\\_eccv\\_2018\\_workshops/w33/html/Xie\\_Pre-training\\_on\\_Grayscale\\_ImageNet\\_Improves\\_Medical\\_Image\\_Classification\\_ECCVW\\_2018\\_paper.html](https://openaccess.thecvf.com/content_eccv_2018_workshops/w33/html/Xie_Pre-training_on_Grayscale_ImageNet_Improves_Medical_Image_Classification_ECCVW_2018_paper.html), [Online; accessed 4. Mar. 2024]

## Appendix

### A1 Results for the ResNet-50 Architecture.

**Table 1.** Comparison between the performance achieved using the ResNet-50 model by our learnt kernel-based averaging method and other transfer learning methods on the test sets of ISIC-2019, APTOS, and RSNA-Pneumonia datasets. MedMerge achieves  $F_1$  performance gains on the ISIC-2019 and APTOS datasets while falling very slightly short on RSNA-pneumonia.

Approach	Source	Target	Acc.	$F_1$
FT	ImageNet	ISIC-2019	0.771	0.634
FT	HAM10K	ISIC-2019	0.803	0.664
LP-FT	ImageNet	ISIC-2019	0.776	0.637
LP-FT	HAM10K	ISIC-2019	0.781	0.642
MedMerge (Ours)	ImageNet+HAM10K	ISIC-2019	<b>0.821</b>	<b>0.709</b>
FT	ImageNet	APTOS	0.837	0.674
FT	EyePACS	APTOS	<b>0.853</b>	0.702
LP-FT	ImageNet	APTOS	0.837	0.685
LP-FT	EyePACS	APTOS	0.852	0.706
MedMerge (Ours)	ImageNet+EyePACS	APTOS	0.850	<b>0.710</b>
FT	ImageNet	RSNA-Pneumonia	0.946	0.944
FT	CheXpert	RSNA-Pneumonia	0.946	0.942
LP-FT	ImageNet	RSNA-Pneumonia	0.936	0.933
LP-FT	CheXpert	RSNA-Pneumonia	<b>0.951</b>	<b>0.948</b>
MedMerge (Ours)	ImageNet+CheXpert	RSNA-Pneumonia	0.945	0.942